

SANDIA REPORT

SAND2004-5101

Unlimited Release

Printed October 2004

A LOW POWER ULTRA-FAST CURRENT TRANSIENT MEASURING DEVICE

P. Rossi, J.P. Sullivan, R.J. Foltynowicz, M. Armendariz, F.J. Zutavern, B.L. Doyle

Prepared by

Sandia National Laboratories

Albuquerque, New Mexico 87185 and Livermore, California 94550

Sandia is a multiprogram laboratory operated by Sandia Corporation,
a Lockheed Martin Company, for the United States Department of Energy's
National Nuclear Security Administration under Contract DE-AC04-94AL85000.

Approved for public release; further dissemination unlimited.



Sandia National Laboratories

Issued by Sandia National Laboratories, operated for the United States Department of Energy by Sandia Corporation.

NOTICE: This report was prepared as an account of work sponsored by an agency of the United States Government. Neither the United States Government, nor any agency thereof, nor any of their employees, nor any of their contractors, subcontractors, or their employees, make any warranty, express or implied, or assume any legal liability or responsibility for the accuracy, completeness, or usefulness of any information, apparatus, product, or process disclosed, or represent that its use would not infringe privately owned rights. Reference herein to any specific commercial product, process, or service by trade name, trademark, manufacturer, or otherwise, does not necessarily constitute or imply its endorsement, recommendation, or favoring by the United States Government, any agency thereof, or any of their contractors or subcontractors. The views and opinions expressed herein do not necessarily state or reflect those of the United States Government, any agency thereof, or any of their contractors.

Printed in the United States of America. This report has been reproduced directly from the best available copy.

Available to DOE and DOE contractors from

U.S. Department of Energy
Office of Scientific and Technical Information
P.O. Box 62
Oak Ridge, TN 37831

Telephone: (865)576-8401

Facsimile: (865)576-5728

E-Mail: reports@adonis.osti.gov

Online ordering: <http://www.osti.gov/bridge>

Available to the public from

U.S. Department of Commerce
National Technical Information Service
5285 Port Royal Rd
Springfield, VA 22161

Telephone: (800)553-6847

Facsimile: (703)605-6900

E-Mail: orders@ntis.fedworld.gov

Online order: <http://www.ntis.gov/help/ordermethods.asp?loc=7-4-0#online>



SAND2004-5101
Unlimited Release
Printed October 2004

A LOW POWER ULTRA-FAST CURRENT TRANSIENT MEASURING DEVICE

P. Rossi, B.L. Doyle, J. Sullivan
Physical and Chemical Sciences Center

R. Foltynowicz
Laser, Optics and Remote Sensing Department

M. Armendariz
RF and Opto Microsystems Department

F. Zutavern
Directed Energy Special Applications

Sandia National Laboratories
PO Box 5800
Albuquerque, NM 87185-1056

Abstract

We have studied the feasibility of an innovative device to sample 1ns low-power single current-transients with a time resolution better than 10 ps. The new concept explored here is to close photoconductive semiconductor switches (PCSS) with a Laser for a period of 10 ps. The PCSSs are in a series along a Transmission Line (TL). The transient propagates along the TL allowing one to carry out a spatially resolved sampling of charge at a fixed time instead of the usual time-sampling of the current. The fabrication of such a digitizer was proven to be feasible but very difficult.

Intentionally Left Blank

Contents

Executive Summary	6
Introduction.....	7
Photoconductive Switches (PCSS).....	8
Digitizer Configurations.....	10
A Small Scale Test.....	11
Second Generation Mask Tests.....	13
Transmission Line Simulation.....	20
Conclusion	22
References.....	24

Figures

1	Layout of the Transient Digitizer.....	7
2	Schematic of Auston's pulse-probe switching experiment.....	8
3	Geometry of the Auston Switch.....	9
4	A Free Running Digitizer.....	11
5	Mask layout of small scale 4-channel transient digitizer prototype	12
6	Four-channels circuit dies	13
7	Samples prepared for transmission and damage threshold testing	14
8	Transmission with linear and semi-log scales	15
9	Visible air breakdown	16
10	Enlargements of the damage spots from samples 1-4.....	17
11	Enlargements of the damage spots from samples 5-9.....	18
12	Transmission features of the 4-channel prototype	20
13	Star Configuration.....	21
14	Attenuation of signal due to DARC 300 coating	22
15	Concept for transiently measuring fusion power	23

Tables

I	Mask Samples for Transmission and Damage Threshold Testing.....	13
II	Sample Transmission at 780 nm	14
III	Summary of Damage Measurements	19
IV	Damage Thresholds	20

Executive Summary

Single pulse transient digitizers are currently only available in the 5 GHz regime. We proposed to develop a digitizer that consists of a number of extremely fast switches placed along the transmission line (TL) and connecting these switches to independent read-out channels, which work in parallel and consist of ‘traditional’ relatively low-speed charge integrators. Our goal is to achieve a 10 ps time resolution in digitizing a 1000 ps transient time range.

Such fast switches have been invented by D.H. Auston and consist of two TLs fabricated on a semi-insulating substrate and separated by a tiny gap. The substrate then becomes conductive when illuminated by a laser’s pulse of suitable frequency, power and duration.

Two switch geometries were found to be practical: a linear design and a star pattern design. The basic notion of our linear transient digitizer have been examined with a small scale 4-channel prototype, including a gold transmission line fabricated on a GaAs substrate in coplanar geometry. The prototype included also a black resist mask superimposed on the circuit. This mask, opaque to the Laser light, features a few openings above the PCSSs, which allow the Laser light to go through and ‘close’ the switches without shorting the remaining circuit. This mask allows a tremendous simplification of the project. With it the laser beam can simply shine uniformly on the whole circuit and standard methods used to manufacture ICs can be employed.

We found that to avoid damage to the masks, laser average and peak power densities should be kept below ~ 1 TW/cm² which is ~ 100 x larger than that required to close the PCSSs. We also performed a study to evaluate the effect of the black plastic DARC 300 (the most successfully of the three we tried) on the attenuation of the signal, which was also shown to be negligible.

Photoconductive Switches look adequate as the basic building blocks of a 100 GHz digitizer. Their switching time is tunable in a range from 0.5 to 10 ps and current ML lasers have enough power to drive a hundred such Auston switches. Two possible transmission line geometries have been studied. A linear geometry with a single TL and many pickup electrodes are suitable for digitizing low current signals (down to 100 μ A), but with a number of samples that can hardly exceed ten due to the substantial signal

A LOW POWER ULTRA-FAST CURRENT TRANSIENT MEASURING DEVICE

Introduction

Single pulse transient digitizers are currently only available in the 5 GHz regime. Sampling at a higher frequency is possible only for periodic signals. We have studied the feasibility of an innovative device to sample 1ns low-power single current-transients with a time resolution better than 10 ps. The transient propagates along a Transmission Line (TL) allowing one to carry out a spatially resolved sampling of charge at a fixed time instead of the usual time-sampling of the current. This amounts to carrying a parallel sampling in n different places with n different electronic channels lowering the sampling time by a factor n . The price for this approach is having a degradation of the signal in its travel along the TL. A purpose of this project is also to evaluate if and under which conditions this degradation is acceptable.

The basic blocks of the digitizer are photoconductive semiconductor switches (PCSS), triggered by a Laser, and are shown schematically in Figure 1.

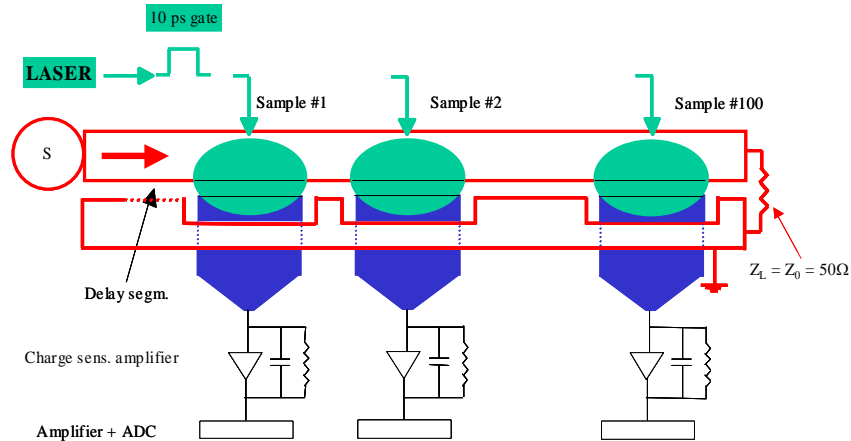


Figure 1. Layout of the Transient Digitizer. (The laser spots are the green ovals.)

Our Transient Digitizer addresses the measurement of low-power single electrical pulses in the frequency range of 100 GHz. Very few other devices are capable of handling a comparable frequency range, but they need high-power periodic signals, which come from the same laser that allows the sampling. But many of the transients important to SNL mission result from single pulses, such as (1) single ion effects in ICs resulting when individual cosmic ray ions strike sensitive areas (IBIC-Ion Beam Induced Charge); (2) the radiation from ICF explosions of DD and DT targets in both Z and in the future NIF. All these transients would require a device like ours.

Finally, our Transient Digitizer is of general usage and might also give rise to patents and large scale industrial applications should technology and price, quite demanding for the time being, become more feasible and affordable in a near future.

Our assessment of the feasibility of this concept is that (1) it appears quite promising for the measurement of ‘high’ current transients (>10 mA), but (2) this approach is still quite speculative for the low current transients involved in cosmic ray effects.

Photoconductive Switches (PCSS)

These switches have been invented by D.H. Auston in early eighties [1] and consist of two TL’s fabricated on a semi-insulating substrate and separated by a tiny gap (see Figure 2). This substrate becomes conductive when illuminated by a laser’s pulse of suitable frequency and power. Lasers capable of short pulses with high power have been available for years and are based on the Mode Locked (ML) technology.

To have the switch closed (conductive) for a very short time one must have both the laser pulse and the substrate carrier lifetime very short. The latter can be obtained several ways, including irradiating the substrate with a dose of low energy protons or neutrons, or by the low temperature’s growth of the substrate.

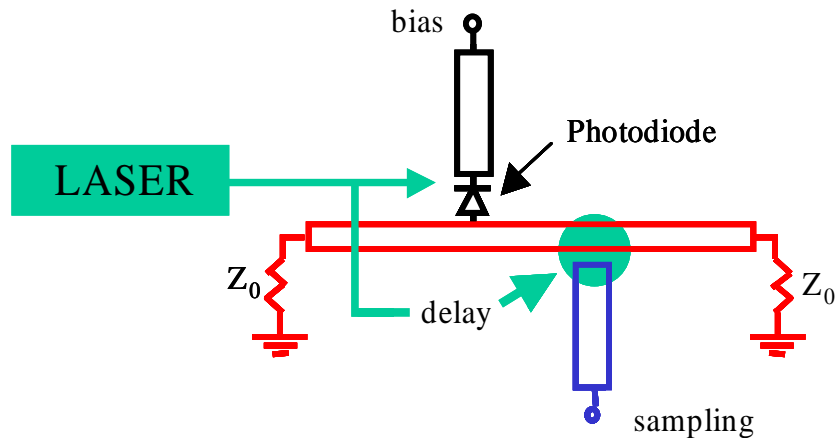


Figure 2. Schematic of Auston’s pulse-probe switching experiment. The circular green area indicates the laser spot that closes the switch.

For example, one of the earlier Auston switches was fabricated on GaAs, irradiated with $3 \cdot 10^{15}$ p(300KeV)/cm², which produced a reduced carrier lifetime of 3 ps and better electrical contacts. The contacts were evaporated Al in a 50 μm microstrip geometry. The switch itself consisted of a 12 μm gap. They employed a ML Rh6G Laser, $\lambda = 580$ nm, 4 ps pulse, 82 MHz rate, 30 pJ/pulse [1].

A vast literature covers the PCSS’s. For example, carrier lifetime definition by Radiation Damage (RD) can be found in [2]. RD-GaAs carrier lifetime of 0.6 ps is obtained with 10^{14} p(200-300 keV)/cm². For more than 10^{12} p/cm² one has lifetime $\propto 1/\text{fluence}$. Also for similar topics see [3].

For carrier lifetime definition by low temperature growing, see [4]. They report the generation of 1-ps infrared ($\lambda = 10.6 \text{ mm}$) pulses employing a GaAs layer (200 nm) grown at 320°C by molecular-beam epitaxy.

For a method to generate short pulses by grounding after diffusion of carriers in an asymmetric pulse, see [5]. They obtain a 0.5 ps electrical pulse using a PCSS with long carrier lifetime, by employing a ML dye laser, with $\lambda = 625 \text{ nm}$ and a 200 fs pulse. They have a 100 μm TL in coplanar geometry, consisting of two 5 μm wide and 1 μm thick Al lines separated by 10 μm (a pulsed TL line and a ground line), fabricated on Si-on-sapphire (SOS) substrate. The Si layer is 0.5 mm thick. The laser spot has to be smaller than the separation between lines and closer to the TL than to the ground line.

For a method to generate a short pulse by grounding through a delayed laser pulse, see [6]. They use a ML Ti:sapphire laser, 80 MHz, $\lambda = 800 \text{ nm}$. As described in Figure 3, they have a TL in coplanar geometry, consisting of lines 20 μm wide, 50-150 nm thick and separated by a 20-40 μm gaps, fabricated onto a semi-insulating GaAs substrate ($\rho = 5 \cdot 10^7 \text{ } \Omega \cdot \text{cm}$). A bias voltage of 45 V is applied. Grounding is delayed by 200 μm thick quartz.

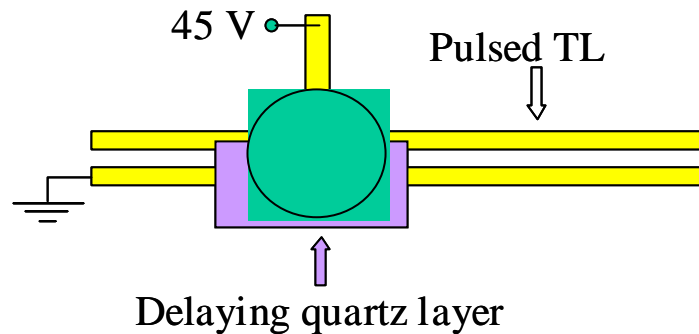


Figure 3. Geometry of the Auston Switch.

Several ML lasers are commercially available. Examples include:

- 1) A solid state Nd:YAG-ML, peak Power 2 kW, $\lambda = 1.064 \text{ mm}$, pulse duration $< 1 \text{ ps}$. The frequency can be doubled to have a $\lambda = 0.532$, suitable to switch on a Ga As PCSS.
- 2) A dye Rhodamine RH6G-ML, 10 kW, $\lambda = 580\text{-}630 \text{ nm}$, pulse duration = 5 ps, repetition frequency = 82 MHz, pulse energy 50 nJ.
- 3) UV-solid state Laser Jenlas (Jenoptiks, Germany), 5 W average, $\lambda = 355 \text{ nm}$, pulse duration $< 10 \text{ ps}$, $f = 85 \text{ MHz}$, pulse energy 60 nJ.
- 4) A Ti_sapphire ML-Laser Mira (Coherent inc.), $\lambda = 700\text{-}980 \text{ nm}$, pulse duration $< 200 \text{ fs}$, $f = 76 \text{ MHz}$, pulse energy 10 nJ (to be employed in our small scale test).

Digitizer Configurations

According to Figure 1, the digitizer consists of a number (let's say 'n') of Auston switches placed along the TL and connecting it to n read-out channels, which work in parallel, and consist of 'traditional' relatively low-speed charge integrators. Our goal is to achieve a 10 ps time resolution in digitizing a 1000 ps transient time range. For that n should be equal to 100. If this proves to be technically too demanding, one could have a lower n and loose either resolution or range.

The configuration of Figure 1 looks possible because Auston switches have already been demonstrated. Of course one has to address further issues, like (1) what is the lowest signal that such a system can measure; (2) how much the signal is going to be degraded in its travel along the transmission line; and (3) how to solve the 'trigger problem'; i.e. how to match the sampling.

(1) The best ultra low noise charge integrators have a noise of about 100 electrons. If we require a signal to noise ratio of 3, then we should have a signal of 300 electrons, which for a gate time of 10 ps would correspond to an average current of 3 A along the read-out channel. The fraction of signal actually conveyed through the switch depends strongly on the switch features and usually is not reported in the literature. A value of 1 over hundred has been suggested by [1], which would bring to 300 A the minimum current that can be sampled. This value is totally approximate and needs further study to be assessed. This value would be barely enough to sample IBIC signals, which range between 100 A and a few mA.

(2) We studied the second issue (signal degradation) both with a computer simulation program (Advanced Design System, Agilent Tech.) and through experimental tests, which have been carried out by employing a small scale prototype (4 channels).

(3) As for the trigger, one has no way to switch off/on a ML Laser with a time resolution better than a few nanoseconds, which can be optically obtained by a Pockels Cell [7]. However, this figure is quite far from what we want to obtain. Actually a ML laser, when switched on with a rather long process, would regularly produce short pulses, lasting 100ps-few ns, with a repetition rate that can approach 100 MHz (for a laser with adequate power). So, there are only the two following ways to have our digitizer 'targeting' the 1 ns transient we would like to analyze.

(1) The first way is to have a 'pulse and probe' experiment, in which the same laser pulse gives rise to the transient one is interested in and then, suitably delayed, would allow the digitization of the same. This is the kind of experiment D.H. Auston and many after him have done to measure phenomena generated by Laser, e.g. for studying photo devices or terahertz pulses, etc. In these experiments the unique Auston switch was able to sample only a small portion of the signal, corresponding to the introduced delay. To sample the whole signal one had to repeat the pulse and probe of the same object many times with different delays. This, although cumbersome, can be done, provided the pulse and probe can actually be repeated on the same object without modifying it. In general, when 'single-pulse phenomena', such as those related to any kind of explosion, are at stake, a more complex digitizer like ours looks necessary.

(2) The second way for recording the transient is to have a Free Running Digitizer shown in Figure 4, which is working for a 'long' time, so as to include the transient, digitizing everything. For example, for digitizing a millisecond period with a time resolution of 10 ps and information of 1 byte per sample one needs a 100 Mbytes RAM per channel and 10 Gbytes for all 100 channels, figures that look reasonable. A Free Running Digitizer is nevertheless a quite demanding project. One should have a hundred channels in IC technology, each one including a charge integrator and an ADC for fast digitizing [8] and [9]. A channel should be able to do its job in a few nanoseconds, before the next laser pulse arrives. Also, if we cannot have more than 100 channels and want nonetheless keep a resolution of 10 ps, we should have a laser hitting every nanosecond with adequate power. With the present laser frequency of 100 MHz, we should multiply by ten the frequency, which in theory might be done splitting the laser beam ten times and suitably delaying each portion. Only a few high-power ML-Lasers can do that. All this looks possible but extremely demanding.

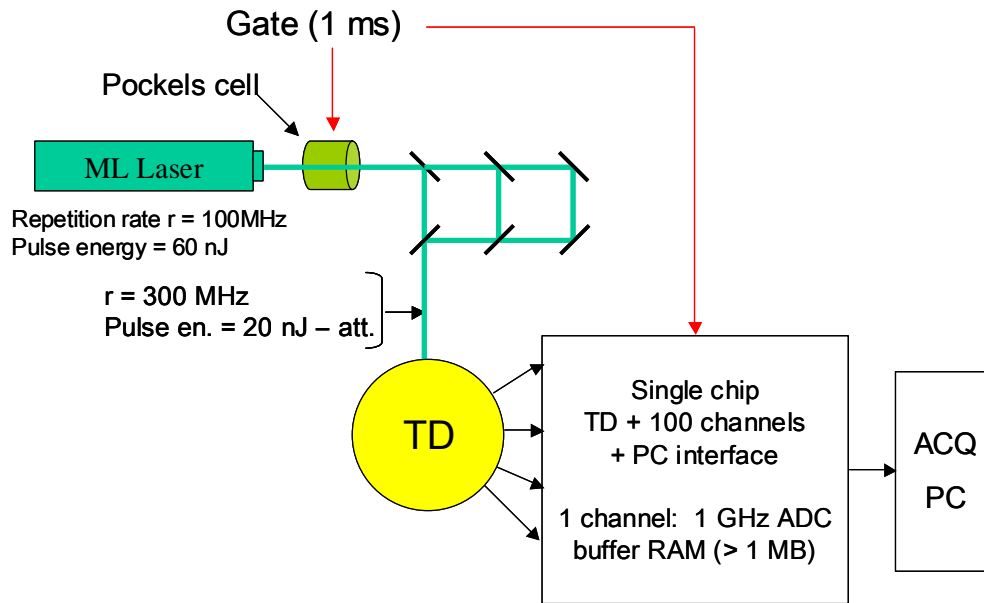


Figure 4. A Free Running Digitizer.

A Small Scale Test

The basic notions of our transient digitizer have been tried with a small scale 4-channels prototype, including a gold transmission line fabricated on a GaAs substrate in coplanar geometry as in Figure 5. The prototype included also a black resist mask superimposed on the circuit. This mask, opaque to the Laser light, features a few openings above the PCSS spots (small square pink spot in Figure 3), which allow the Laser light to go through and close the switches without shorting the remaining circuit. This mask allows a tremendous simplification of the project: with it the laser beam can simply shine uniformly on the whole circuit, ameliorating special 'optics' to convey the light only to the switches. Although individual laser channels are still possible in a small scale test, such an optical system would be totally

unworkable in a digitizer with a large number of channels. Figure 6 shows circuit's dies produced by lithographic process with and without black layer.

Several tests have been carried out to try a few materials as an opaque plastic capable to stand high-power laser pulses. In fact, it is known that materials with a high absorption coefficient for low intensity light might change their behavior when hit by high intensity light. In the latter case they might be no longer able to absorb the light. This phenomenon, called photo-bleaching, is due to a saturation of the absorbing material's atomic levels excitation. The plastics examined are produced by the manufacturer Brewer Science, Rolla, Missouri 65401 and are (1) PSKTM 1000, Photosensitive Black Matrix; (2) DARC 300 Black Polyimide; (3) DARC 102 Black Polyimide. A micron thickness of the three materials has a Transmittance < 1% for ~ 800 nm, steady, low-power light.

For this test, we employed a Ti-sapphire ML-Laser Mira (Coherent inc.), with $\lambda = 800$ nm, pulse duration < 200 fs, $f = 76$ MHz, and pulse energy 10 nJ. A micron thick material showed the following Transmittance for the three materials: (1) 3.0%, (2) 1.7%, and (3) > 80%. So DARC 300 looks the best suited to avoid photo-bleaching.

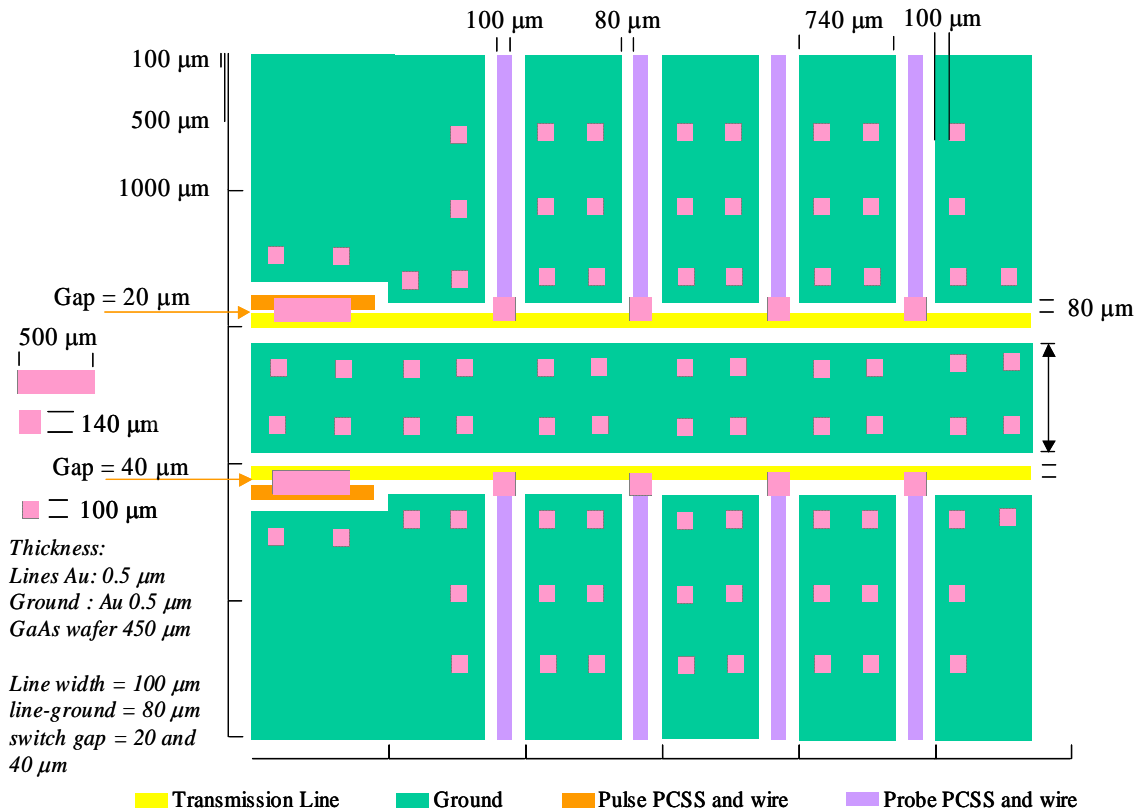


Figure 5. Mask layout of small scale 4-channel transient digitizer prototype.

In Figure 5, a small scale prototype in coplanar geometry. Small pink square spots represent the openings in the superimposed opaque mask. The smaller ones have been introduced for allowing the wire bonding between different portions of the ground, while the bigger spots correspond to the PCSS.

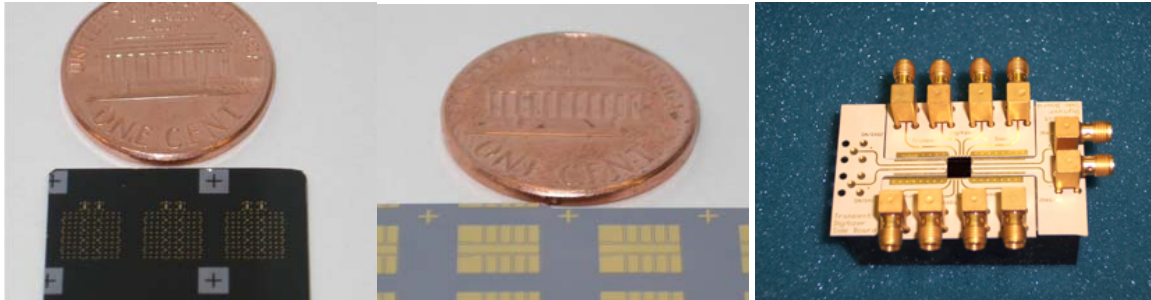


Figure 6. Four-channels circuit dies with and without the black resist cover, and fully packaged into the prototype test device.

Second Generation Mask Tests

A second generation of mask samples was prepared on glass slides for transmission and damage threshold testing. Three preparations of the spin-on plastics (PCK1000, DARC 102, and DARC 300) were produced for a total of nine samples shown in Table I and Figure 7. A spectrophotometer was used to measure transmission over the wavelength range of 0.2 to 3.5 μm (UV to IR). The results are shown in Figure 8 and Table II.

Table I. Mask Samples for Transmission and Damage Threshold Testing.

	PSK1000, 200 C, 90 sec	DARC 102, 150 C, 90 sec	DARC 300, 150 C, 90 s
500 rpm	1	2	3
1000 rpm	4	5	6
1000 rpm X 2	7	8	9

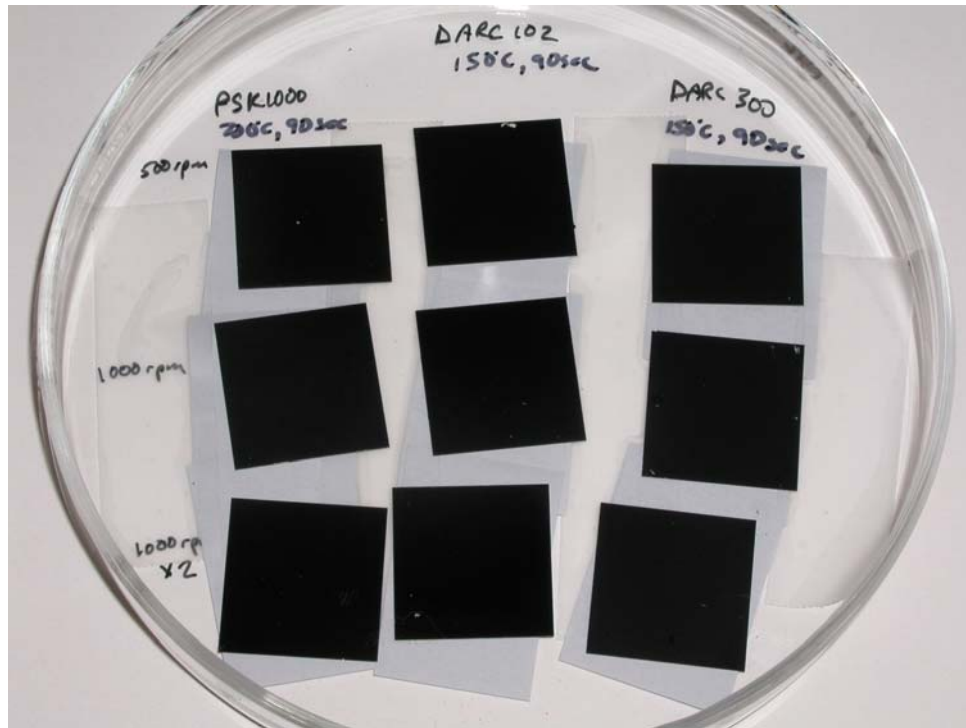


Figure 7. Nine samples prepared for transmission and damage threshold testing.

Table II. Sample Transmission at 780 nm.

1	0.344
2	38.24
3	0.01
4	2.16
5	59.57
6	0.87
7	0.935
8	45.07
9	0.01

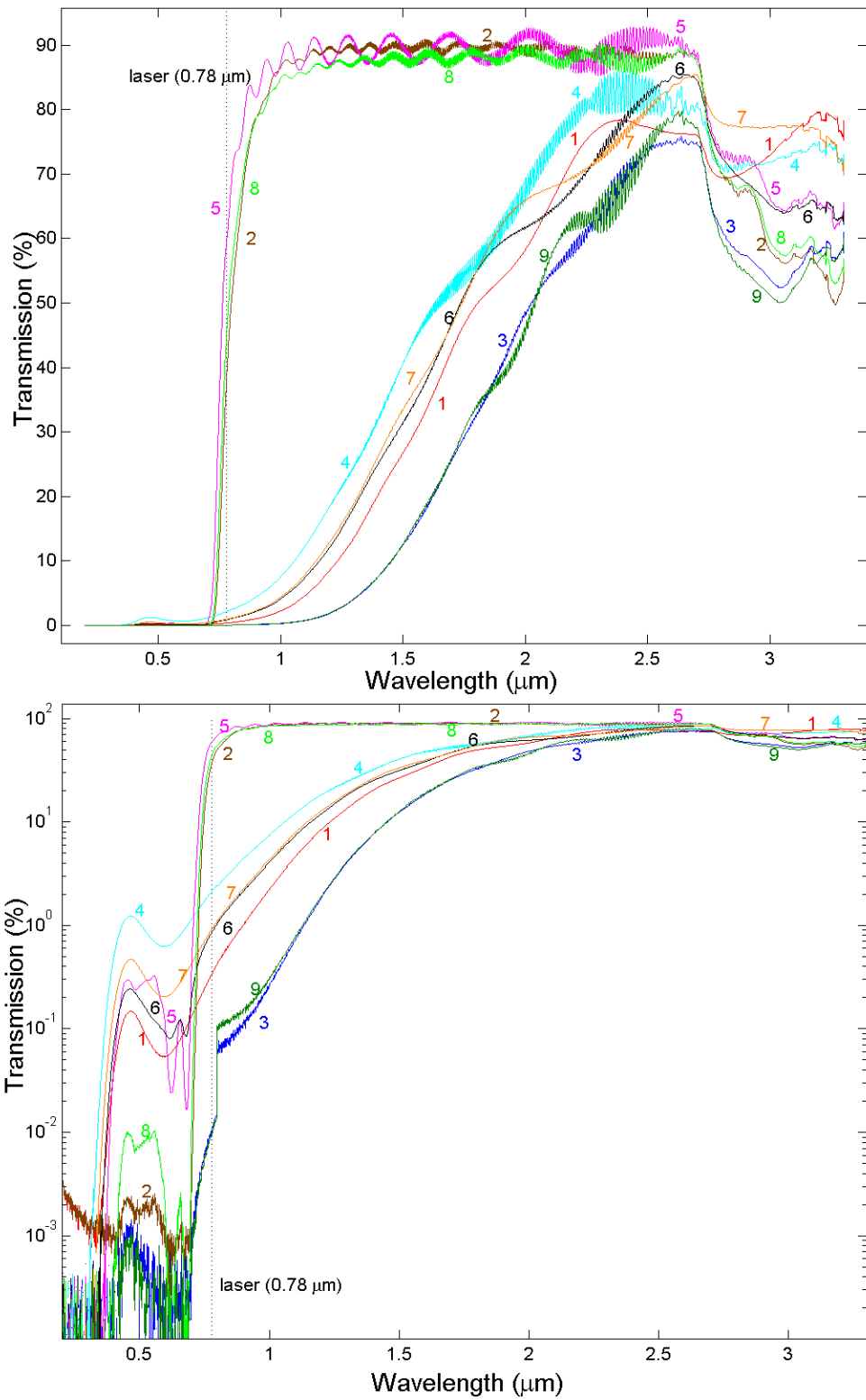


Figure 8. Transmission is shown with linear (top) and semi-log (bottom) scales for the 9 mask samples of Table I.

Damage threshold measurements were made with a 780 nm, 140 fs, chirped pulse amplified, mode-locked, fiber laser that delivers 1.5 mJ per pulse at 1 kHz. The laser beam was focused to approximately 50 μm in diameter. The beam energy was attenuated to 50 μJ , where air breakdown was clearly visible at the focus (Figure 9). The small visible focus was positioned exactly on the surface of a sample. The laser beam was blocked, attenuated with neutral density filters, and the sample was moved to a new position along a line perpendicular to the beam path. While monitoring the laser beam through the sample with a high sensitivity power meter, the laser beam was unblocked for approximately 10 s. At low energies no change in the transmitted power was observed, although microscopic inspection revealed some surface damage. At moderate energies, the transmitted power decreased and surface damage was observed. At higher energies, the transmitted power increased. The results are shown in Figures 10-11 and Table III. The average and peak power densities, below which no change in transmission was observed are shown in Table IV. In many cases, a gradual change to a new value of transmitted energy was observed while the laser beam was illuminating the samples. This could be explained in two ways: (1) an average power thermal effect, or (2) a cumulative damage effect due increased damage with each short pulse. Since the time between laser pulses was 1 ms, we speculate that it was probably the latter. However, no attempt has been made to verify this speculation. To avoid damage to the masks, laser average and peak power densities should be kept below the values shown in Table IV or $\sim 1 \text{ TW}/\text{cm}^2$. Typical laser powers required to operate a 100x100 micron Auston switch are in the 10MW/cm² range. These results therefore indicate that the black resist masks tested here should perform well in this application, because the power required to operate the switch is $\sim 100\text{x}$ smaller than that required to damage the mask.

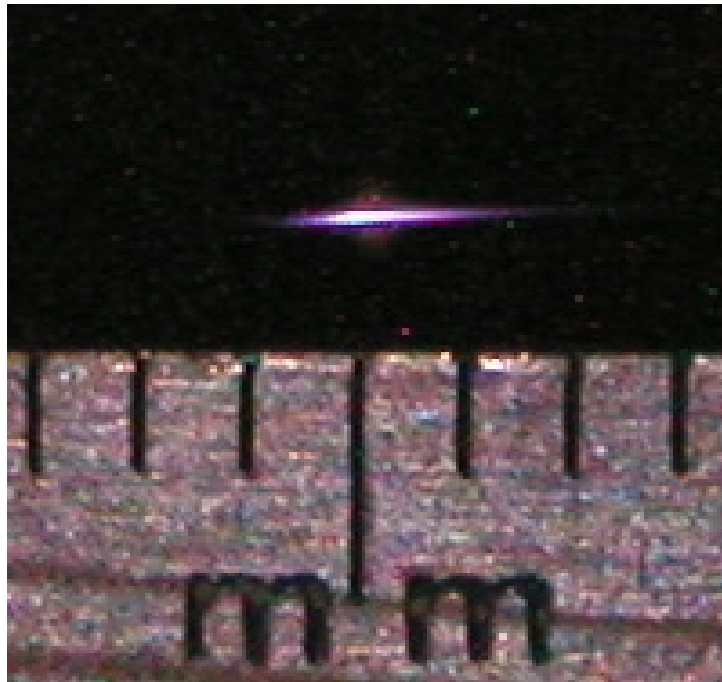


Figure 9. The visible air breakdown shown at the focus of the laser in this photograph was used to position the beam on the samples.

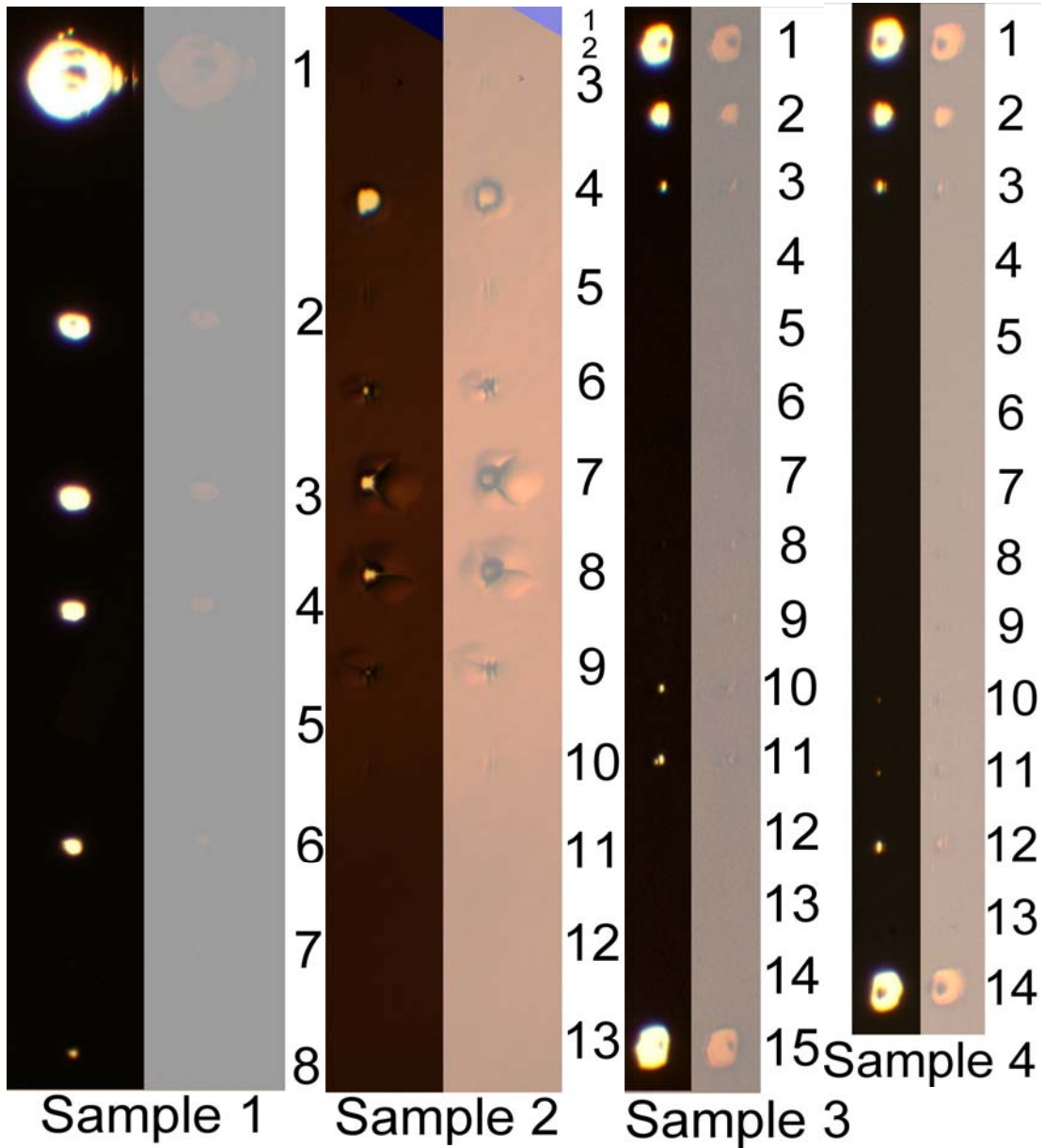


Figure 10. Enlargements of the damage spots from samples 1-4 are shown in these pictures. The samples were illuminated from behind (left) to show transmission and from above (right) to enhance the visibility of the surface damage.

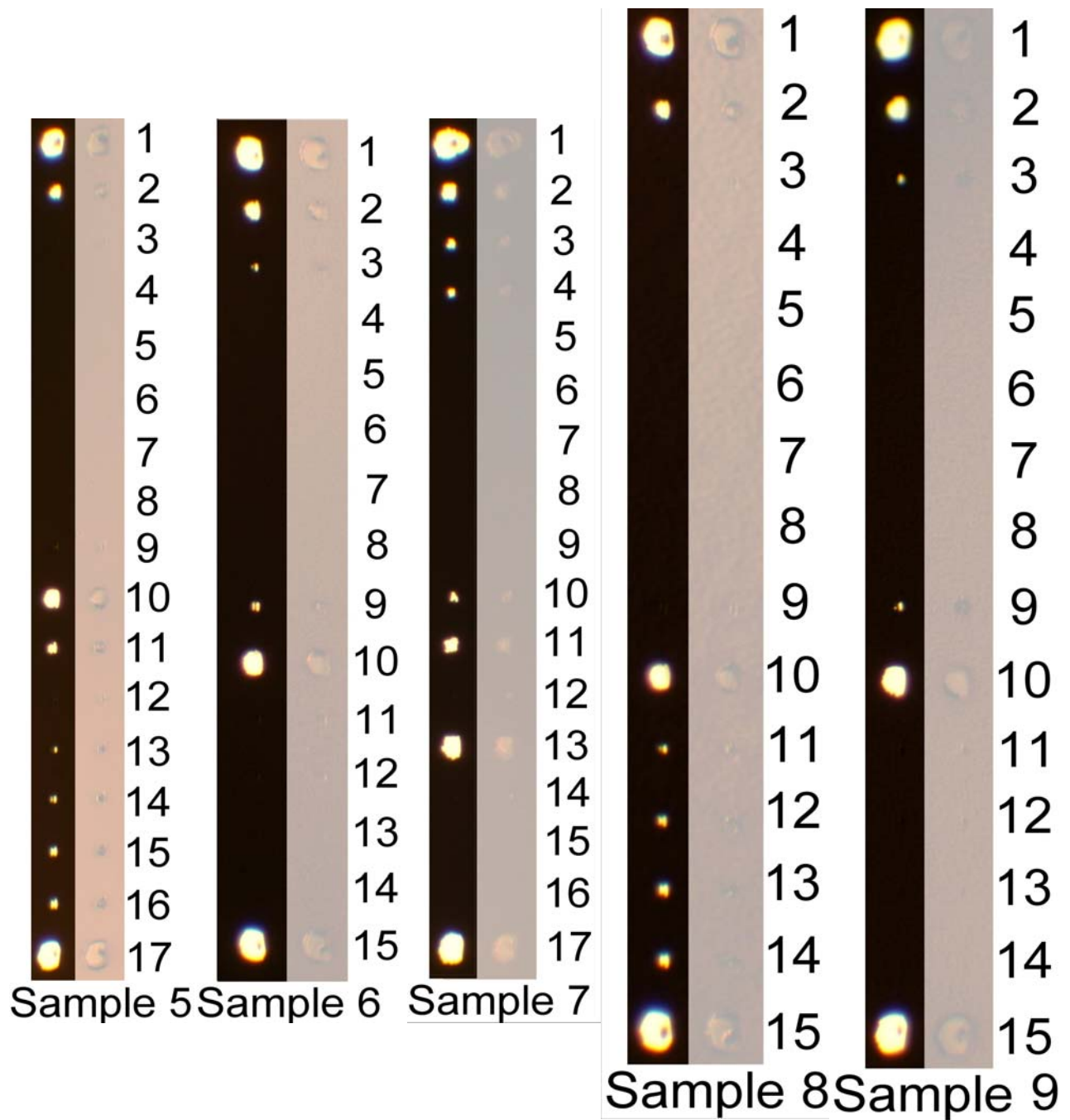


Figure 11. Enlargements of the damage spots from samples 5-9 are shown in these pictures. The samples were illuminated from behind (left) to show transmission and from above (right) to enhance the visibility of the surface damage.

Table III. Summary of Damage Measurements Made on All Samples.

	Avg Power		Energy		damage dia.	Power Density
	(mW)	(μJ)	(μm)	(TW/cm ²)		
sample 1						
spot 1	197	197	400	71.67		
spot 2	59	59		21.46		
spot 3	29	29		10.55		
spot 4	9.78	9.78		3.56		
spot 5	2.37	2.37		0.86		
spot 6	6.53	6.53		2.38		
spot 7	3.41	3.41		1.24		
spot 8	4.08	4.08	60	1.48		

	Avg Power		Energy		damage dia.	Power Density
	(mW)	(μJ)	(μm)	(TW/cm ²)		
sample 2						
spot 1	0.163	0.163		0.06		
spot 2	0.63	0.63		0.23		
spot 3	2.66	2.66		0.97		
spot 4	8.02	8.02	50	2.92		
spot 5	2.88	2.88		1.05		
spot 6	4.17	4.17		1.52		
spot 7	5.21	5.21		1.90		
spot 8	4.97	4.97		1.81		
spot 9	3.65	3.65	5	1.33		
spot 10	2.62	2.62		0.95		
spot 11	0.942	0.942		0.34		
spot 12	0.226	0.226		0.08		
spot 13	0.059	0.059		0.02		

	Avg Power		Energy		damage dia.	Power Density
	(mW)	(μJ)	(μm)	(TW/cm ²)		
sample 3						
spot 1	50.6	50.6	110	18.41		
spot 2	8.02	8.02		2.92		
spot 3	2.61	2.61		0.95		
spot 4	0.631	0.631		0.23		
spot 5	0.941	0.941		0.34		
spot 6	1.19	1.19		0.43		
spot 7	1.36	1.36		0.49		
spot 8	1.62	1.62		0.59		
spot 9	1.7	1.7		0.62		
spot 10	2.61	2.61		0.95		
spot 11	2.87	2.87		1.04		
spot 12	0.228	0.228		0.08		
spot 13	0.064	0.064		0.02		
spot 14	0.06	0.06		0.02		
spot 15	50.6	50.6		18.41		

	Avg Power		Energy		damage dia.	Power Density
	(mW)	(μJ)	(μm)	(TW/cm ²)		
sample 4						
spot 1	50.6	50.6	105	18.41		
spot 2	8.02	8.02		2.92		
spot 3	2.61	2.61		0.95		
spot 4	0.631	0.631		0.23		
spot 5	0.164	0.164		0.06		
spot 6	0.228	0.228		0.08		
spot 7	0.941	0.941		0.34		
spot 8	1.19	1.19		0.43		
spot 9	1.36	1.36		0.49		
spot 10	1.62	1.62		0.59		
spot 11	1.7	1.7	12.5	0.62		
spot 12	2.61	2.61		0.95		
spot 13	0.06	0.06		0.02		
spot 14	50.4	50.4		18.33		

	Avg Power		Energy		damage dia.	Power Density
	(mW)	(μJ)	(μm)	(TW/cm ²)		
sample 5						
spot 1	50.6	50.6	115	18.41		
spot 2	8.02	8.02		2.92		
spot 3	2.61	2.61	11	0.95		
spot 4	0.631	0.631		0.23		
spot 5	0.164	0.164		0.06		
spot 6	0.06	0.06		0.02		
spot 7	0.228	0.228		0.08		
spot 8	0.941	0.941		0.34		
spot 9	2.87	2.87		1.04		
spot 10	18.83	18.83		6.85		
spot 11	6.16	6.16		2.24		
spot 12	2.87	2.87		1.04		
spot 13	3.66	3.66		1.33		
spot 14	4.16	4.16		1.51		
spot 15	4.97	4.97		1.81		
spot 16	5.21	5.21		1.90		
spot 17	50.3	50.3		18.30		

	Avg Power		Energy		damage dia.	Power Density
	(mW)	(μJ)	(μm)	(TW/cm ²)		
sample 6						
spot 1	50.6	50.6	105	18.41		
spot 2	8.02	8.02		2.92		
spot 3	2.61	2.61		0.95		
spot 4	0.631	0.631		0.23		
spot 5	0.164	0.164		0.06		
spot 6	0.06	0.06		0.02		
spot 7	0.228	0.228		0.08		
spot 8	0.941	0.941		0.34		
spot 9	2.87	2.87		1.04		
spot 10	18.83	18.83		6.85		
spot 11	1.7	1.7		0.62		
spot 12	1.62	1.62	4	0.59		
spot 13	1.36	1.36		0.49		
spot 14	1.19	1.19		0.43		
spot 15	49.6	49.6		18.04		

	Avg Power		Energy		damage dia.	Power Density
	(mW)	(μJ)	(μm)	(TW/cm ²)		
sample 7						
spot 1	50.6	50.6		18.41		
spot 2	8.02	8.02		2.92		
spot 3	2.61	2.61		0.95		
spot 4	2.61	2.61		0.95		
spot 5	0.631	0.631		0.23		
spot 6	0.164	0.164		0.06		
spot 7	0.06	0.06		0.02		
spot 8	0.228	0.228		0.08		
spot 9	0.941	0.941		0.34		
spot 10	2.87	2.87		1.04		
spot 11	6.16	6.16		2.24		
spot 12	1.7	1.7		0.62		
spot 13	18.83	18.83		6.85		
spot 14	1.62	1.62		0.59		
spot 15	1.36	1.36		0.49		
spot 16	1.19	1.19		0.43		
spot 17	49.3	49.3		17.93		

	Avg Power		Energy		damage dia.	Power Density
	(mW)	(μJ)	(μm)	(TW/cm ²)		
sample 8						
spot 1	50.6	50.6		18.41		
spot 2	8.02	8.02		2.92		
spot 3	2.61	2.61		0.95		
spot 4	0.631	0.631		0.23		
spot 5	0.164	0.164		0.06		
spot 6	0.06	0.06		0.02		
spot 7	0.228	0.228		0.08		
spot 8	0.941	0.941		0.34		
spot 9	2.87	2.87		1.04		
spot 10	18.83	18.83		6.85		
spot 11	3.66	3.66		1.33		
spot 12	4.16	4.16		1.51		
spot 13	4.97	4.97		1.81		
spot 14	5.21	5.21		1.90		
spot 15	49.2	49.2		17.90		

	Avg Power		Energy		damage dia.	Power Density
	(mW)	(μJ)	(μm)	(TW/cm ²)		
sample 9						
spot 1	50.6	50.6		18.41		
spot 2	8.02	8.02		2.92		
spot 3	2.61	2.61		0.95		
spot 4	0.631	0.631		0.23		
spot 5	0.164	0.164		0.06		
spot 6	0.06	0.06		0.02		
spot 7	0.228	0.228		0.08		
spot 8	0.941	0.941		0.34		
spot 9	2.87	2.87		1.04		
spot 10	18.83	18.83		6.85		
spot 11	1.7	1.7		0.62		
spot 12	1.62	1.62		0.59		
spot 13	1.36	1.36		0.49		
spot 14	1.19	1.19		0.43		
spot 15	49.2	49.2		17.90		

Table IV. Damage Thresholds (max. power density showing no change in transmission).

sample	Power Density	
	Average (W/cm ²)	Peak (TW/cm ²)
1	173.16	1.24
2	264.83	1.89
3	86.58	0.62
4	132.42	0.95
5	254.65	1.82
6	86.58	0.62
7	86.58	0.62
8	185.89	1.33
9	86.58	0.62

Transmission Line Simulation

We employed the Advanced Design System software by Agilent Inc. to evaluate the transmission features of the 4-channel prototype. Graphs like that in Figure 12 below have been obtained.

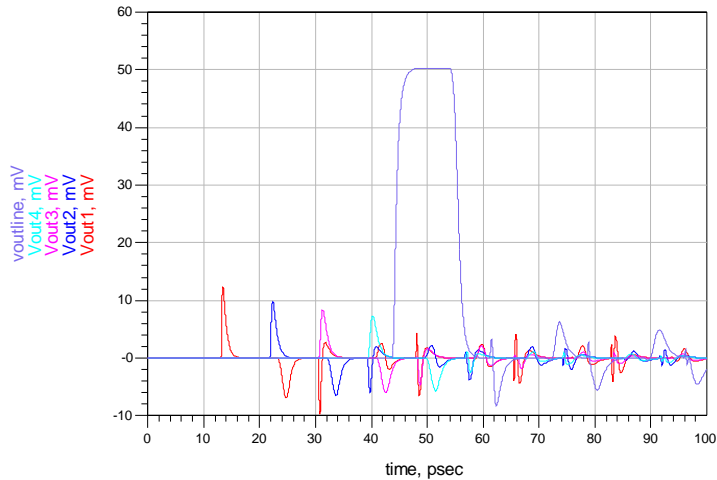


Figure 12. Transmission features of the 4-channel prototype.

The graph shows the signal induced on the different pickup electrodes placed along the TL. Each color corresponds to a different electrode: first electrode (red), second electrode (blue), third electrode (violet), fourth electrode (very light blue) and the end of TL (light blue). In the simulation, the input signal was a sharp square wave of 10 ps that arrives attenuated at TL's end. The PCSSs (gap = 100 μm) are open (no laser light) and the induced signals are merely due to electrical induction of the charge moving along the Transmission Line. One notes the substantial

attenuation of signal along the line (something like 15% every 1 mm (10 ps)) and also important reflections due to the pickup electrodes' presence. This analysis shows that only a limited number of switches are actually acceptable and that a hundred switches can surely not be handled.

To solve this issue, we are currently studying a different configuration of the sampling circuit, which foresees the splitting of the signal in n different TLs (the Star Configuration shown in Figure 13). Each TL then can be sampled through just one PCSS and no important degradation of signal would take place. This would work only if the signal is split in a perfectly evenly way, which has not yet been demonstrated. Further tests are under way. However, the minimum signal that can be measured by this method is n times bigger than that by a linear configuration, so the method is not adequate for very low signal like IBIC.

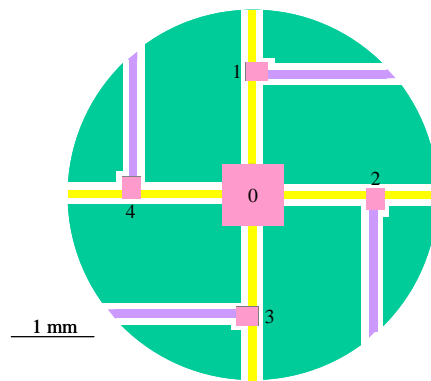


Figure 13. Star Configuration. In '0' there is the signal source.

Finally, we performed a further study to evaluate the effect of the black plastic DARC 300 (the most successfully of the three we tried) on the attenuation of the signal, and these results are plotted in Figure 14. Taking into account the resistivity and the dielectric constant of this plastic, we obtained the next graph, which represents the signal loss due to a 1 mm transmission coplanar line with and without DARC 300. The line looks the same up to 20 GHz and then one sees .25 to .4 dB difference at the higher end. The calculation is only good up to 40 GHz and beyond that the error is greater. That's why the data looks noisier in that region. The lines were measured using an HP8510 vector analyzer with Cascade coplanar waveguide probes. The probes were launched on one of the 1 mm transmission lines of the transient digitizer which has the 150 micron probes. The negligible attenuation change introduced by DARC 300, together with the previous test showing this has negligible photo-bleaching, suggest this is an ideal candidate as a cover mask for our circuit and strongly support the feasibility of the project.

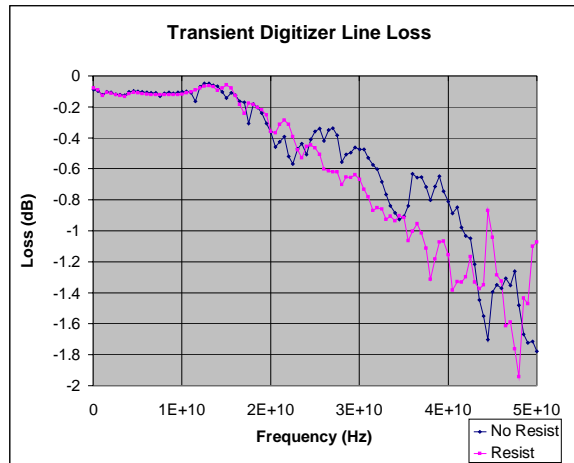


Figure 14. Attenuation of signal due to DARC 300 coating.

Conclusion

Photoconductive Switches look adequate as basic building blocks of a 100 GHz digitizer. Their switching time is tunable in a range from 0.5 to 10 ps and current ML lasers have enough power to drive a hundred such “Auston” switches. Two possible transmission line geometries have been studied. A linear geometry with a single TL and many pickup electrodes are suitable for digitizing low current signals (down to 100 A) but with a number of samples that can hardly exceed ten due to the substantial signal degradation that each pickup electrode implies. A Star Configuration can handle a hundred time samples, but the initial signal cannot be smaller than 10s of mA. This latter configuration might not be suitable for IBIC experiments, where signals rarely exceed a few mAs. As for ICF explosions, their energy should be adequate also for a star geometry.

Pulse and probe experiments look feasible simply by extending the 4-channels test circuit we already prepared. The external low speed readout channels can be connected through suitable capacitors and wire-bonding. If a Free Running Digitizer is wanted, parallel readout channels have to operate at 1 GHz and IC technology is required. The cost of a 10 channel circuit, which would be the next step to undertake, has been estimated to be between \$200,000 and \$300,000. We have also demonstrated the adequacy of a black plastic mask, built with lithographic techniques, to stop the laser light everywhere but the openings for the PCSSs. This achievement would allow ICs with a hundred switches or even a million of them, if required in other applications different from the transient digitizer of this project. For example, a vast number of switches with 10 ps resolution could be part of an optical matrix to record images of particularly fast phenomena.

The basic notion of this project, i.e. having a parallel sampling in different probing spots, can have other applications. For example, a transient of gamma rays can be recorded. Such a transient (17 MeV gammas) is produced by the DD and TT nuclear fusion reactions in ICF

facilities like the NIF at Lawrence Livermore and the Z-Machine at Sandia. A heavy metal bar, gold for example, facing the gamma beams at an angle, can convert the gammas in e^-e^+ pairs. According to Figure 10, the gamma rays hitting the upper part of the bar would arrive earlier than those hitting the lower part, establishing a proportionality between position along the bar and time. A sample of the charge generated by the gammas would offer a graph of fusion power as a function of time, which is information of paramount importance. The required time resolution for such a measurement is 10-20 ps, and a sampling method based on photoconductive switches would be ideal.

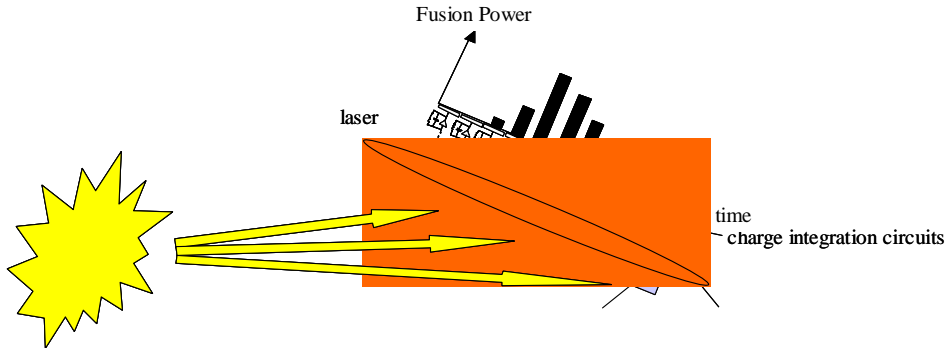


Figure 15. Concept for transiently measuring the fusion power of a Z or NIF DT implosion where the intensity of the fusion gamma rays are detected.

Finally, the careful reader will notice that we didn't actually test the prototype during this one-year LDRD project. This resulted because much of our progress was at the end of fiscal year 2004, and the circuit boards were not received until the very last week. In addition, an improved mask design for the metallization was submitted, but not received this FY. These original and improved prototype 4-channel transient digitizers are now ready for testing. All that is required is a smallish (\$40K) LDRD, and we could complete these tests.

References

1. D.H. Auston et al, Appl. Phys.Lett. 41(7),1982, p. 599
2. M.B. Johnson et al., Appl. Phys. Lett. 54(24).1989, p.2424
3. A.Y. Elezzabi et al., Appl. Phys. Lett. 66 (4), 1995, p.402
4. A.Y. Elezzabi et al., Optics Letters, 19 (12), 1994, p.898
5. D. Kroekel et al., Appl. Phys. Lett. 54 (11), 1989, p. 1046
6. J.F. Holzman et al., Appl. Phys. Lett. 76(2), 2000, p. 134.
7. The fastest way to do that is optically through a Pockels Cell (Electro Optic effect): > 3 ns (on->off) (LINOS-Photonics, Q-switch Driver HVD 1000).
8. 2 GHz PMC (PCI Mezzanine Card), 10 bits, 32 MB buffer, (for radar). Delphi, Eng. Group, Costa Mesa, CA 92627, tel (949) 515 1490.
9. High-resolution ADC, 19.6 GHz clock frequency (for radar), 6000 Josephson junction second-generation chip, Mukhanov et al., in Superconductor Sci. and Tech., IOP electronic journals, 2001 and HYPRES Inc.

Intentionally Left Blank

Distribution:

- 1 F. D. McDaniel
University of North Texas
Department of Physics
PO Box 305370
Denton TX 76203-5370
- 1 P. Rossi, Professor
University of Padova
Dipartimento di Fisica
Via Marzolo 8
35131 Padova, ITALY
- 1 MS 0123 D.L. Chavez, 01011
1 MS 0601 J.A. Simmons, 01120
1 MS 0874 M. Armendariz, 01751
1 MS 1056 B.L. Doyle, 01111
1 MS 1153 F. Zutavern, 15333
1 MS 1415 J.C. Barbour, 01110
1 MS 1421 G.A. Samara, 01130
1 MS 1421 J.P. Sullivan, 01112
1 MS 1423 R.J. Foltynowicz, 01128
1 MS 1427 J.M. Phillips, 1100
- 1 MS 9018 Central Technical Files, 8945-1
2 MS 0899 Technical Library, 9616